A Novel Tapered Rotating Electrical Machine Topology Utilizing Cut Amorphous Magnetic Material

Nesimi Ertugrul[1], Ryusuke Hasegawa[2], *Fellow, IEEE*, Wen L. Soong[1], John Gayler[3], Stephen Kloeden[3], and Solmaz Kahourzade[1]

[1]School of Electrical and Electronic Engineering, The University of Adelaide, Adelaide, SA 5005, Australia
[2]Metglas Inc., Conway, SC 29526 USA
[3]GMT Ltd., Adelaide, SA 5008, Australia

Amorphous magnetic materials (AMMs) have been used in low-frequency power transformer applications for more than two decades but not commercially utilized in high-frequency rotating electrical machines despite their low iron losses, which is an order of magnitude lower than conventional silicon iron. This was primarily due to the lack of a suitable handling method and an economical cutting technique. This paper reports a novel brushless synchronous permanent magnet rotating electrical machine that combines the benefits of the previous machine topologies while offering higher torque (due to the larger air-gap surface area compared with the flat axial-field machine) and ease of manufacturing from AMM material, which is suitable for a range of high-efficiency, high-power density, and high-speed machine applications. This paper provides the details and the performance characteristics of this novel tapered-field AMM machine as a generator at high speeds using a bonded rotor magnet topology.

Index Terms— **Amorphous magnetic materials (AMMs), tapered-field brushless permanent magnet machine.**

I. Introduction

THE conventional silicon steel-based magnetic cores primarily used in rotating electrical machines have a laminated form with a thickness of between 0.1 and 0.6 mm and are mainly restricted to radial field 2-D designs. However, even high-quality silicon iron has significantly high iron losses specifically when considered in high-speed motor/generator applications.

In Fig. 1(a), a loss comparison graph for silicon iron and an emerging magnetic material, amorphous magnetic material (AMM) as a function of operating frequency is given. The corresponding BH loops are given in Fig. 1(b) [1] and illustrate that AMM's iron (or core) losses are typically an order of magnitude lower than conventional silicon iron. This is particularly an advantage at higher operating frequencies as in variable-speed motor drives. Note that the saturation flux density for AMM (∼1.6 T) is significantly lower than silicon steel (such as 2.2 T for M19) [2]; however, its permeability is one or two orders of magnitude higher.

AMM has been used in power transformers for more than two decades, which commonly operate at low frequencies and do not require complex cut shapes. Although a substantial reduction in iron losses may be achieved if AMM material could be used in conventional radial-field rotating machine topologies, they are not suitable for cut AMM construction. This is due to these topologies involving a large number of complex slots, which have to be accurately cut.

A key issue with using AMM in rotating machines has been the difficulty of cutting AMM accurately and economically to achieve the complex stator structures, due to its extreme hardness and its handling limitations before and after cutting, and also assembly limitations. These problems have recently been solved [3], [4], which led to a novel

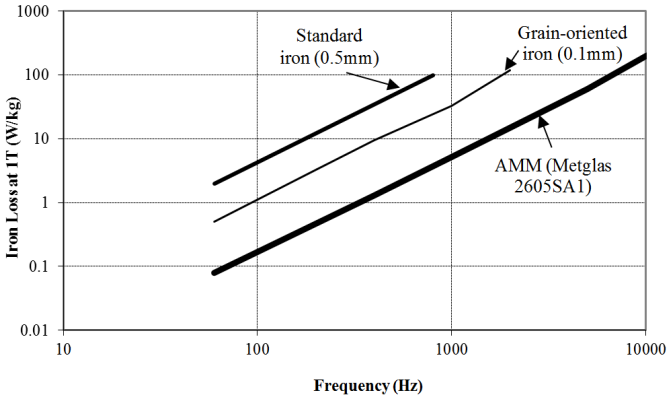

(a)

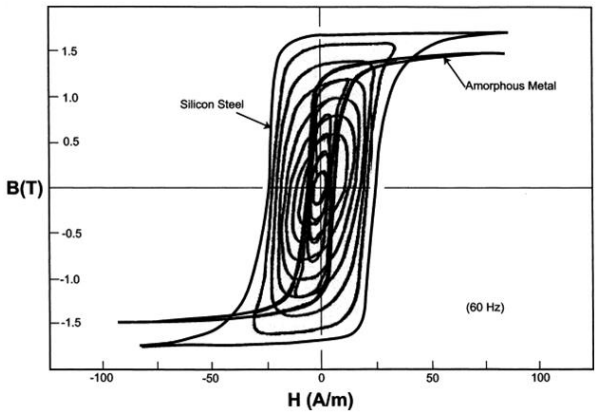

(b)

Fig. 1. (a) Typical iron loss versus frequency characteristics of silicon-iron and AMM core materials. (b) BH loops at 60 Hz for silicon iron and AMM [1].

Manuscript received October 9, 2014; revised December 28, 2014 and January 19, 2015; accepted January 20, 2015. Date of publication February 3, 2015; date of current version June 26, 2015. Corresponding author: N. Ertugrul (e-mail: nesimi@eleceng.adelaide.edu.au).

Color versions of one or more of the figures in this paper are available online at http://ieeexplore.ieee.org.

Digital Object Identifier 10.1109/TMAG.2015.2399867

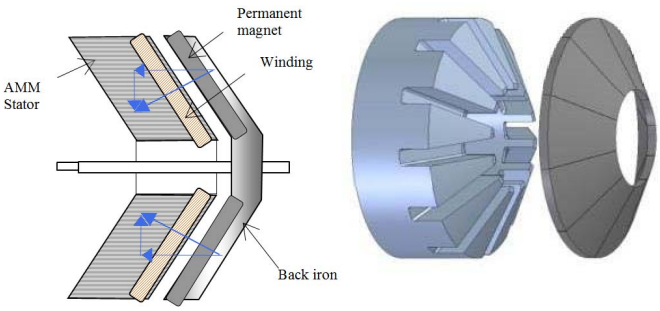

Fig. 2. Left: cross-sectional view of the novel AMM brushless permanent magnet motor topology. Right: 3-D view of the stator core with open slots and the rotor magnet structure.

rotating machine topology with a tapered stator core and rotor [5]. This significantly reduced the manufacturing cost, which was the largest barrier preventing commercialization of AMM in rotating electrical machine applications. This novel machine topology also suits the limited ribbon width of commercially available AMM laminations (currently a maximum of 212 mm) and hence reduces material wastage.

Fig. 2 shows the proposed electric machine structure, where, the stator iron is highlighted with its laminations, the magnets are shown with a dark fill, and the windings are highlighted with a diagonal line pattern. The arrows indicate the direction of the major components of the magnetic flux flow. It is important to note that unlike the conventional radial and axial machine topologies, the flux flow in this tapered-field design includes both radial and axial-field components.

Note that the tapered-field design is not suitable for conventional silicon-iron laminated structures due to the larger thickness of the silicon-iron material, which limits the formation of a smooth stator structure.

The literature survey performed on angled electric motors [6]–[9] revealed that previous studies were primarily focused on improving the electromagnetic performance and use silicon iron material, but without considering their manufacturing benefits. For example, Demag's brake motor uses axial force in its braking mechanism, and axial force is integral to the Electrotechnical Institute's rotary-percussive mechanism [6] to provide both rotary and axial motion. In addition, NovaTorque's hybrid design [7] provides a motor with additional benefits over conventional axial-field motors, including higher torque, improved thermal performance, and simpler windings. Note also that the use of the hybrid shape in NovaTorque's design changes the flux path from that of a conventional machine, leading to the removal of back iron. However, such a design increases the complexity of both manufacture (as it requires different-sized laminations stacked together) and construction (assembling the stator poles together). In these previous hybrid studies, an angled rotor is combined with an angled stator to maintain a uniform air gap. However, the switched reluctance machine by General Electric Company [8] with a single bearing combines an angled rotor with a conventional cylindrical stator to produce an uneven air gap to reduce the radial force and the effect of eccentricity on the rotor. This offers protection against the rotor and stator making contact.

A sandwich-type dual-rotor flat axial-field AMM rotating machine has also been reported recently in [10] and [11]. The topology described in these studies included two different AMM-based stator pole piece structures, which were obtained by wrapping (with a final slit to reduce eddy-current loss) and by cutting (to obtain a pole piece made from various sized AMM laminations). The preformed windings and the AMM pole pieces are then encapsulated to form a complete stator sandwiched between two permanent magnet rotors. Although the concept machines have demonstrated high-efficiency operation, the rigidity of the stator structure and handling/manufacturing/assembly cost of the pole pieces have not been assessed and reported. In addition, high-speed operation and heat dissipation characteristics of the concept machines have not been investigated, which are critical for commercial products.

The topology proposed in this paper is novel due to the utilization of cut AMM in the core, the structure of both the stator and the rotor, and the manufacturing steps involved for practical and economical cutting of AMM. Therefore, the primary contributions of this paper are in the area of the new machine topology, the magnetic design of the proposed configuration that requires a 3-D analysis approach, and the definition of the manufacturing steps for an energy-efficient rotating AMM machine for commercial use.

The rest of this paper is organized as follows. In Section II, the novel machine structure is explained. In Section III, a set of simulated and experimental studies are presented to demonstrate the characteristics of the prototype machine while operating at high speeds as a generator. Section IV concludes this paper.

II. Analysis of the Novel AMM Machine

A characteristic feature of the stator of the novel AMM machine topology is that its taper angle θ offers an exit path for the waterjet beam used to cut the stator slots. From the geometry, it can be shown that the minimum taper angle $\theta_{\min}$ is a function of the slot depth d_s and the stator inner diameter D_i

$$\theta_{\min} = \tan^{-1}\left(\frac{d_s}{D_i}\right). \tag{1}$$

The cutting process developed in this paper produces cuts with smooth edges with no material degradation up to a maximum cutting thickness [5]. Therefore, the thickness of the tape-wound AMM core and the available ribbon width are important to define the maximum size of a tapered-field stator structure, which can be cut. Commercially sensitive studies indicate that cutting is economical below a certain thickness and with certain slot profiles. However, it is possible to develop larger diameter AMM machines for high-power output, which can be obtained using a nested structure, or alternatively, the same motor structure can be duplicated on a common shaft.

A. Production Methods of Tapered Field AMM Machine

The principal manufacturing steps of the new AMM machine stator topology are shown in Fig. 3 and explained as follows: 1) the unannealed and uncoated AMM ribbon is wound to a tapered shape [Fig. 3(a)] as tightly as possible to

(a) (b)

Fig. 3. Principal manufacturing steps of the novel AMM machine. (a) Tapered AMM stator core before cutting. (b) After the core is cut with abrasive waterjet technology.

achieve maximum stacking factor; 2) the core is annealed to improve the material properties after the stresses produced by the winding process of the core; 3) the core is impregnated to insulate the surface of the tape wound AMM core; 4) the cutting of the slots is performed using a custom built jig and abrasive waterjet technology [Fig. 3(b)]; and 5) the stator winding is inserted. Note that the mechanical stress during this process will result in increased iron loss and can affect the impregnation process which needs to be considered during manufacturing process.

B. Magnet and Air-Gap Characteristics

The magnet working radius (air-gap radius) sets the torque arm for an electric motor and is directly related to the torque production. The larger this radius is, the more torque the motor produces. In general, an optimized radial motor has an average magnet working radius of 0.25 D_e (the motor external diameter). For flat-axial motors, the magnet working radius is more difficult to define as the radius varies over the area of the air gap and varies by magnet shape. For disk magnets, the magnet working radius can be approximated as 0.3 D_e. If pie-shaped magnets are used (Fig. 2), it increases to ∼0.35 D_e. The proposed tapered-field machine has a magnet working radius similar to that of the flat-axial motor.

Assuming that the shear stress is constant and the air-gap radii are the magnet working radii as defined above, the torque of motor is proportional to the total magnet surface area (MSA) (or total possible air-gap area). For the proposed tapered-field design, the total MSA is determined by the taper angle. Fig. 4 shows the relationship between the effective MSA and the angle of the stator and rotor assuming a constant external diameter (D_e). The shapes of the tapered-field machine corresponding to the angles of 30° and 60° are also shown in the figure. Note that the effective MSA increases rapidly as the angle increases. For example, for an angle of 60°, the MSA (and hence torque) is 100% greater than that of the conventional flat axial-field machine (0°) for the same outer diameter. For the angles of 30° and 45°, the MSA increase is ∼15% and 40%, respectively.

III. Concept Design and Experimental Studies

A. Concept Design

The concept novel AMM machine has been analyzed using a 3-D finite-element (FE) design tool, and an open-slot stator

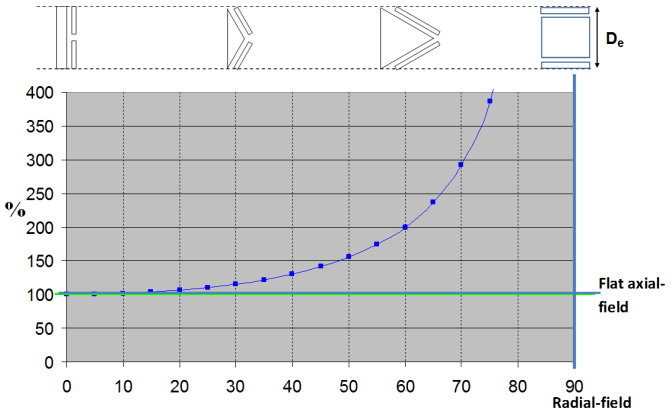

Fig. 4. Calculated MSA for tapered-axial machine versus conventional (flat) axial machine.

TABLE I
Dimensions, Key Parameters, and Mass Breakdown of the Concept Tapered AMM Machine

Machine Specifications	
Torque	2.8 Nm
DC voltage	380 V
Speed	7000 rpm
Airgap	0.7 mm
Measured phase resistance	0.19 Ω
Measured phase inductance	0.489 mH
Rotor	
Number of poles	10
Core material	Steel 4140
Permanent magnet type	Bonded NdFeB
Magnet thickness	6 mm
Magnet remanent flux density	0.71 T
Magnet conductivity	0 S/m
Total magnet weight	276 g
Complete rotor weight	1590 g
Stator	
Outer diameter/inner diameter	110 mm/ 45 mm
Width of AMM ribbon	30 mm
Stator taper angle	25°
(Minimum taper angle	21 °)
Number of slots	12
Slot depth	17 mm
Material	2605SA1, annealed
Core cross-sectional area	975 mm^2
Net core weight	1086 g
Total weight of the copper windings	440 g
Winding turns per phase	96
Winding type	double-layer concentrated and star connected

and tapered rotor topology were built to study the performance characteristics of the machine. The machine specifications are provided in Table I, including the mass breakdown and magnet specifications. A relatively low taper angle of 25° for the stator was used for the concept demonstration as the focus was primarily on the proof of the manufacturing approach. From (1), the minimum taper angle for this design is ∼21°.

Fig. 5 shows a cutaway view of the novel machine topology, where half of the rotor magnets and the stator windings are removed for clarity. The prototype machine utilized an open-slot stator structure, and the rotor included 10 bonded NdFeB surface-mounted permanent magnets with a tapered back iron.

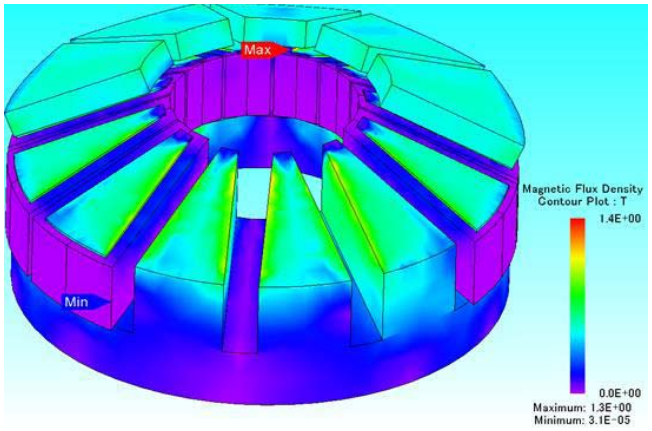

Fig. 5. Calculated magnetic flux density distribution of the prototype design under no-load conditions.

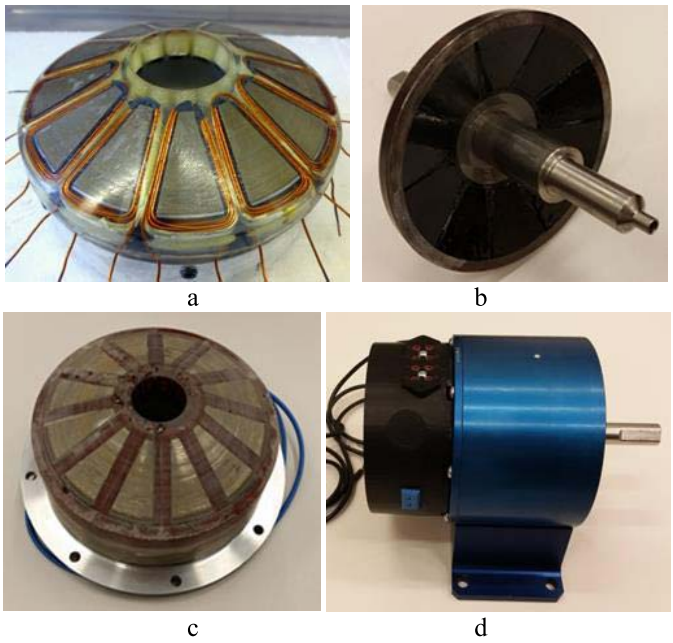

Fig. 6. Basic components of the prototype machine. (a) Tapered stator with windings. (b) Ten pole rotor with bonded NdFeB magnets of 6 mm thickness. (c) Stator with back support. (d) Assembled prototype fully enclosed without any cooling.

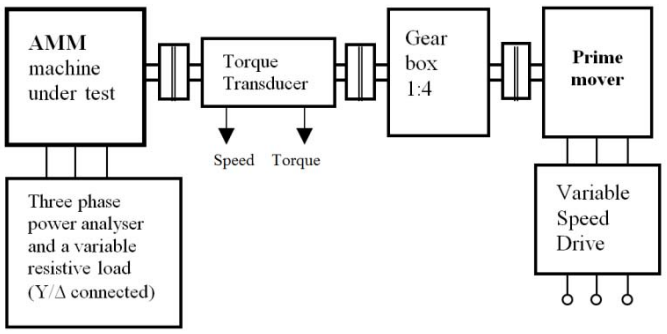

Fig. 7. Block diagram of the custom-built high-speed dynamometer setup to test the novel AMM machine.

A concept demonstration machine has been built to verify the FE design study and also to investigate the accuracy of cutting and the limitations of slot number and size, and the magnet types (sintered or bonded NdFeB).

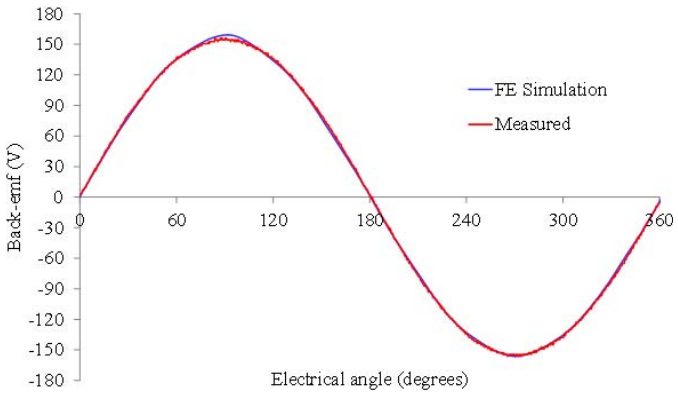

Fig. 8. Measured and FE simulated back EMF waveforms at 7000 r/min.

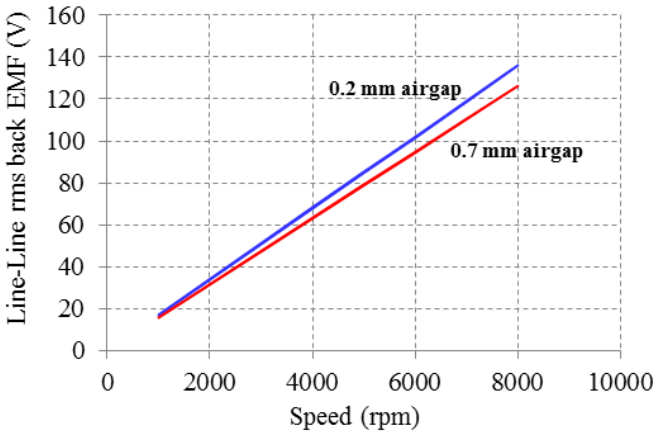

Fig. 9. Measured line back EMF voltage for different air-gap lengths.

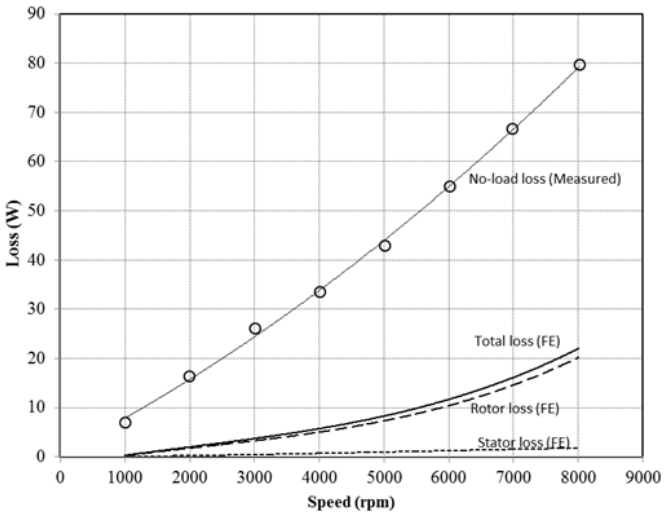

Fig. 10. Measured no-load power loss and FE calculated stator and rotor open-circuit losses up to 8000 r/min.

Fig. 6 shows the winding assembly in the completed cut stator [Fig. 6(a)] and the bonded magnet rotor assembly [Fig. 6(b)] of the concept demonstrator. The quality of the tapered stator with windings and the slot cutting accuracy can be observed from the photos. The finished stator [Fig. 6(c)] and the rotor are assembled in a fully enclosed aluminum housing [Fig. 6(d)] with bearings to complete the prototype machine.

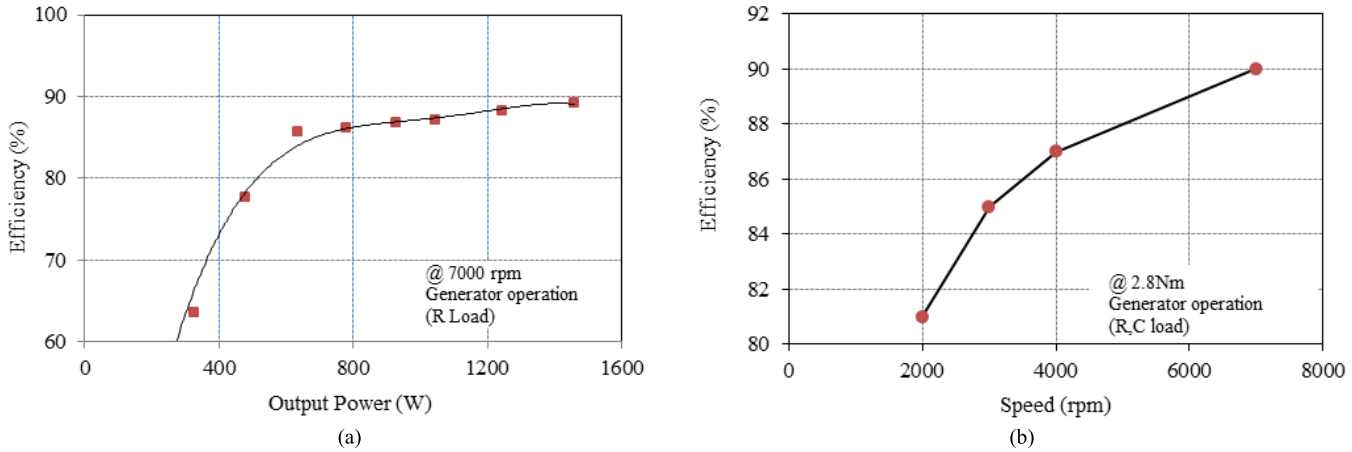

Fig. 11. Measured efficiency characteristics. (a) As a function of output power at 7000 r/min. (b) As a function of speed at 2.8 Nm.

B. Test Setup and Results

A high-speed dynamometer setup has been developed to test the final prototype machine as a generator. The components of the test setup are shown in Fig. 7.

During the tests, the AMM machine was run as a generator, driven by a variable-speed 10 kW induction motor drive and a gear box up to a maximum speed of 8000 r/min and loaded by three-phase resistive and capacitive adjustable load banks. The shaft torque and the speed is measured by an in-line torque transducer, and the load power is measured by a power analyzer. The measured dc voltage drops across two phases when a dc current was applied and was used to calculate the stator resistance of one phase of the machine (0.19 Ω). An external ac voltage source was used to excite the terminals of the machine to measure its impedance and hence the inductance (0.489 mH).

Fig. 8 shows that the machine has a sinusoidal back electromotive force (EMF) waveform and there is a good correspondence between the measured and the calculated shape. The back EMF is sensitive to the axial air-gap length, as shown in Fig. 9. It was observed that as the air gap gets larger, the efficiency is higher at low powers but lower at high powers. An air gap of 0.7 mm was used for the remaining tests on the machine.

Fig. 10 shows the measured no-load power losses obtained by measuring the torque under open-circuit conditions up to 8000 r/min. It also shows the calculated rotor and stator open-circuit loss components of the test machine. As the conductivity of the bonded magnet is close to zero, the magnet loss is assumed negligible.

Two possible sources of extra losses, which could explain the large discrepancies between the measured and the predicted no-load losses, are bearing losses (friction and preload) and rotor losses. Friction and preload losses are significantly higher in this single air-gap design due to the large attractive axial force between the rotor and the stator [12]. A dual air-gap design, which should have significantly lower axial forces and hence bearing losses, will be investigated in the future. In addition, the use of open stator slots can cause potential for high rotor losses. The design uses bonded rotor magnets which have high resistivity and so low losses, however, does have a solid steel back iron which may be another potential loss mechanism to be investigated.

The measured efficiency versus output power characteristic at 7000 r/min is shown in Fig. 11(a). The efficiency was still increasing at the maximum tested output power of ∼1.5 kW and reaches nearly 90%. At this operating point, the loss is ∼185 W and thus the 50 W discrepancy between the calculated and the measured no-load loss in Fig. 10 at 7000 r/min shows that there is significant room for efficiency improvement.

Additional tests have also been done to determine the efficiency characteristics of the concept machine at lower operating speeds. For instance, efficiencies approaching 90% were achieved at a speed of 2000 r/min at output powers of ∼200–300 W. Fig. 11(b) shows the measured efficiency characteristic of the machine as a function of speed at full load, at 2.8 Nm. Although further efficiency improvements are possible, the efficiency characteristic given in Fig. 11 is already very close to the existing EU's super premium efficiency limits for sinusoidal machines at the power rating considered. Note the efficiency of the power converter would also need to be considered.

The thermal design of the concept demonstrator machine was not optimized and does not have any forced cooling. Thus, it produced a relatively low shear stress of ∼8 kPa. However, a substantial level of improvement is expected with improved thermal design, which is currently under investigation.

The electric loading of the concept design is in the order of 36 kA/m (rms). The torque per electromagnetic unit mass of the design is ∼0.9 Nm/kg. The average magnetic loading is found to be ∼0.23 T, which is relatively low due to the bonded magnets, the stray air gaps from the use of flat magnets on a circular back iron, and the open stator slot design. This will be further investigated to increase it to more typical levels using curved sintered magnets and a semiclosed stator slot topology.

IV. Conclusion

This paper described a novel tapered-field topology for AMM machines, which is suitable for waterjet cutting. It has a rigid structure suitable for high-speed operation and offers the potential for high-output torque for a given outer diameter.

The main benefit of the proposed tapered machine design is to allow convenient manufacturing with AMM to seek to utilize its potential for low stator iron loss. Otherwise, its performance in terms of quantities, such as efficiency and torque/unit mass, is expected to be comparable with an axial-field machine with similar air-gap area and magnet volume. The tapered design does allow a larger air-gap area for the same outer diameter but also has a longer axial length.

A demonstration machine with a 25° tapered open-slot stator core was analyzed with 3-D FE software. It was constructed to validate the proposed manufacturing approach and to obtain the electrical characteristics. The prototype machine used standard 30 mm AMM ribbon and was cut using a precision waterjet cutting technology. This prototype also allowed investigating the accuracy of cutting and the major loss components in the machine.

The novel machine topology demonstrated an efficiency approaching 90% with a 0.7 mm air gap at 7000 r/min. It was also found that the machine maintains this high efficiency at lower operating speeds. A larger dynamometer test setup has been built to investigate the maximum power limit of the machine, which will be done after developing improving cooling for the machine.

The proposed machine topology could be used in high-efficiency and high-speed machine applications, including high-speed pumps, flywheels, vehicles, home appliances, and in portable generators.

Further areas of investigation of this novel AMM machine design will include using: 1) the semiclosed stator slots to reduce magnet losses; 2) a dual stator/rotor structure to reduce bearing forces and hence losses; 3) a higher taper angle to increase output torque for a given stator diameter; 4) a nested arrangement for higher power machines; 5) the alternative rotor configurations for field weakening operation; and 6) a switched reluctance design to eliminate the magnet requirement.

ACKNOWLEDGMENT

This work was supported by the Australian Research Council under Grant LP0455574. The authors would like to thank G. Liew, C. Tang, I. Linke, and M. Ainslie for their contributions to the project over the last 10 years.

REFERENCES

[1] R. Hasegawa, "Applications of amorphous magnetic alloys," *Mater. Sci. Eng., A*, vols. 375–377, pp. 90–97, Jul. 2004.

[2] *Vehicle Technologies Program, Annual Progress Report for the Advanced Power Electronics and Electric Machinery Technology Area*, U.S. Department of Energy, Washington, DC, USA, Jan. 2008.

[3] G. S. Liew, N. Ertugrul, W. L. Soong, and J. Gayler, "Investigation of axial field permanent magnet motor utilising amorphous magnetic material," *Austral. J. Elect. Electron. Eng.*, vol. 3, no. 2, pp. 111–119, 2007.

[4] G. S. Liew, N. Ertugrul, W. L. Soong, and J. Gayler, "An investigation of advanced magnetic materials for axial field brushless permanent magnet motor drives for automotive applications," in *Proc. 37th IEEE Power Electron. Specialists Conf. (PESC)*, Jeju, Korea, Jun. 2006, pp. 1–7.

[5] J. A. Gayler, S. R. Kloeden, R. Hasegawa, and N. Ertugrul, "Method of constructing core with tapered pole pieces and low-loss electrical rotating machine with said core," U.S. Patent 8 726 490 B2, Aug. 18, 2011.

[6] O. N. Veselovskii, A. M. Yarunov, S. A. Shvers, and S. L. Sternina, "The action of an asynchronous conical motor used as a rotary-percussive mechanism," *J. Mining Sci.*, vol. 4, no. 2, pp. 197–199, 1968.

[7] J. P. Petro and K. G. Wasson, "Rotor-stator structure for electrodynamic machines," U.S. Patent 7 061 152, Jun. 13, 2006.

[8] E. A. Fisher and E. Richter, "Conical rotor for switched reluctance machine," U.S. Patent 5 233 254, Aug. 3, 1993.

[9] A. G. Flogvall, "Motor arrangement comprising at least three co-planar conical motors," U.S. Patent 4 628 220, Dec. 9, 1986.

[10] Z. Wang *et al.*, "Development of a permanent magnet motor utilizing amorphous wound cores," *IEEE Trans. Magn.*, vol. 46, no. 2, pp. 570–573, Feb. 2010.

[11] Z. Wang *et al.*, "Development of an axial gap motor with amorphous metal cores," *IEEE Trans. Ind. Appl.*, vol. 47, no. 3, pp. 1293–1299, May/Jun. 2011.

[12] K. Sitapati and R. Krishnan, "Performance comparisons of radial and axial field, permanent-magnet, brushless machines," *IEEE Trans. Ind. Appl.*, vol. 37, no. 5, pp. 1219–1226, Sep./Oct. 2001.

Nesimi Ertugrul (M'95) received the B.Sc. degree in electrical engineering and the M.Sc. degree in electronic and communication engineering from Istanbul Technical University, Istanbul, Turkey, in 1985 and 1989, respectively, and the Ph.D. degree from the University of Newcastle, Newcastle upon Tyne, U.K., in 1993.

He has been with The University of Adelaide, Adelaide, SA, Australia, since 1994, where he is currently an Associate Professor. He has authored a book entitled *LabVIEW for Electric Circuits, Machines, Drives, and Laboratories* (Prentice-Hall, 2002). His current research interests include sensorless operation and design of permanent magnet machines utilizing emerging magnetic materials and variable speed drives, renewable energy systems, power quality monitoring and condition monitoring, and energy storage.

Ryusuke Hasegawa (F'86) was born in Nagoya, Japan. He received the B.Eng. and M.Eng. degrees in electrical science from Nagoya University, Nagoya, in 1962 and 1964, respectively, and the Ph.D. degree in materials science from the California Institute of Technology, Pasadena, CA, USA, in 1969.

He was with the California Institute of Technology, IBM T. J. Watson Research Center, Yorktown Heights, NY, USA, AlliedSignal, Inc., Morristown, NJ, USA, and Honeywell International, Morristown. He is currently with Metglas Inc., Conway, SC, USA, as the Vice President of Research and Development. His current research interests include magnetism and magnetic materials in amorphous and nanocrystalline materials.

Wen L. Soong (S'89–M'93) was born in Kuala Lumpur, Malaysia. He received the B.Eng. degree from The University of Adelaide, Adelaide, SA, Australia, in 1989, and the Ph.D. degree from the University of Glasgow, Glasgow, U.K., in 1993.

He was with the General Electric Corporate Research and Development Center, Schenectady, NY, USA. He joined The University of Adelaide in 1998. His current research interests include permanent magnet and reluctance machines, renewable energy generation, and condition monitoring.

John Gayler received the B.Sc. (Hons.) degree in chemical engineering from the University of Adelaide, Adelaide, SA, Australia, in 1963.

He was involved in a number of multinational organizations predominantly in automotive parts with supply chain management. He retired in 2001. His current research interests include innovation and product development involving amorphous magnetic materials, and the areas of building advanced manufacturing in energy efficient products.

Stephen Kloeden held a trade qualification as a fitter/turner with the water supply industry in 1990. He was with the School of Mechanical Engineering, University of Adelaide, Adelaide, SA, Australia, where he was involved in related engineering enterprises, including eight years of experience. He joined GMT Ltd., Adelaide, as part of the Amorphous Magnetic Material Product Development Team, in 2001, where he is involved in cutting process and product development activities.

Solmaz Kahourzade (S'11–M'12) was born in Bandar Abbas, Iran, in 1984. She received the B.S. degree in electronics engineering from the K. N. Toosi University of Technology, Tehran, Iran, in 2007, and the M.Eng. degree in electrical power engineering from the University of Malaya, Kuala Lumpur, Malaysia, in 2012. She is currently pursuing the Ph.D. degree with The University of Adelaide, Adelaide, SA, Australia.

She has authored or co-authored over 20 papers in international journals and conferences. Her current research interests include modeling and design of electrical machinery.